International Journal of Thermophysics, Vol. 10, No. 6, 1989

The Use of a Novel Capillary Flow Viscometer for the Study of the Argon/Carbon Dioxide System

A. Hobley,[1] G. P. Matthews,[1] and A. Townsend[1]

Received March 28, 1989

A novel capillary flow viscometer has been constructed which is ultimately intended to be used for the measurement of the viscosities of corrosive gases such as hydrogen chloride up to pressures of 0.1 MPa. In the process of checking the accuracy of the instrument, we have measured the viscosities of carbon dioxide and argon/carbon dioxide mixtures relative to standard argon viscosities in the temperature range 301 to 521 K. The carbon dioxide viscosities have previously been used to determine a "viscosity average" well depth for the gas, which is an essential parameter for the Chapman–Enskog analysis of the argon/carbon dioxide mixture viscosities as described here. The argon/carbon dioxide interaction viscosities which result from this analysis are compared to corresponding values calculated from the mixture viscosities of Kestin and Ro, and to Mason-Monchick calculations performed by Maitland et al., using the potential energy surface of Pack et al. The interaction viscosities are also used to calculate diffusion coefficients, which are compared to Mason–Monchick diffusion coefficients of Maitland et al. and to diffusion coefficients calculated from the mixture viscosities of Kestin and Ro. An inverted isotropic potential is used to calculate second virial coefficients, which are compared with experiment and with calculations based on the potential energy surface of Hough and Howard and of Parker et al.

KEY WORDS: carbon dioxide; diffusion; gas mixtures; inversion; potential function; virial coefficients.

1. INTRODUCTION

The transport properties of gases, in particular their viscosities, have proved to be an important source of information in the study of intermolecular forces. The interactions of monatomic species are now well

[1] Chemistry Division, Department of Environmental Sciences, Plymouth Polytechnic, Drake Circus, Plymouth PL4 8AA, United Kingdom.

0195-928X/89/1100-1165$06.00/0

840/10/6-5

known [1], and attention is currently focused on atomic/diatomic interactions such as argon/carbon dioxide [2–10] and argon/hydrogen chloride [11–14]. A novel gas viscometer has been constructed [15] and used for the measurement of carbon dioxide and argon/carbon dioxide viscosities. The viscometer is currently being used for the study of argon/hydrogen chloride mixtures.

The measurements of carbon dioxide viscosities, and their use in the calculation of a spherically averaged potential for this gas, are described elsewhere [16]. The use of Chapman–Enskog theory based on the assumption that the carbon dioxide molecule is spherical yields a "viscosity average" isotropic potential. It has been shown by Maitland et al. [17] that while this does not correspond to any geometrically representable average over the interactions between two molecules, the isotropic potential is nevertheless a legitimate method of representing the molecular interactions. Moreover, within the same approximation framework, the carbon dioxide well depth ε derived from the isotropic potential (i.e., the maximum attractive energy $-\varepsilon$ ascribable to the pseudospherical interaction energy U) can be used for the calculation of a well depth for the Ar/CO_2 interaction.

A potential energy surface for the Ar/CO_2 system has been calculated by Pack and his collaborators [4–7] using an electron gas model. Maitland et al. [8] have recognized argon/cabon dioxide interactions as being highly anisotropic and suitable for the testing of various averaging methods for converting anisotropic to isotropic potential functions. These functions express the interaction energy U as a function of the separation r between the center of each atom or molecule. The averages were compared to viscosities calculated from the Pack potential energy surface [4, 6] using the Mason–Monchick approximation. Their survey showed that the best averaging process is that of a "locus average" based on a $U(r)$, $r^{1/2}$ locus for viscosity, although difficulties were encountered near positions of minimum potential energy. However, inversion of second virial coefficients for argon/carbon dioxide yielded a significantly different isotropic potential energy function. The present interaction viscosities, and corresponding diffusion coefficients, are compared with the Mason–Monchick calculations used in the averaging survey. Second virial coefficients calculated from the isotropic potential presented here are compared to experimental values in the light of the conclusions of Maitland et al.

Hough and Howard [10] have recently calculated a potential energy surface for Ar/CO_2 using a modification of their corrected Born–Oppenheimer approximation. This approximation is partly analogous to the infinite-order sudden approximation but is more robust under conditions of slow radial motion. They point out the uncertainty arising from the fact

that two very different electron gas potentials calculated by Pack et al. [4, 5] both reproduce certain experimental data, in particular second virial coefficients.

2. EXPERIMENTAL

The viscosities of mixtures of argon and carbon dioxide were measured using a newly constructed capillary flow viscometer shown in Fig. 1, which has been fully described in a previous publication [15]. For the non-corrosive system Ar/CO_2, the apparatus was used in a traditional configuration. The differential pressure transmitter and front vessel were isolated, and the gas sample was contained in the mercury manometer itself. Both the manometer and the back vessel were maintained at 30.0°C, and connected via a coiled capillary tube enclosed in an oil bath of accurately controlled temperature. Measurements were made of the times for the gas mixture to pass from the manometer to the back vessel, with a known pressure difference across the capillary tube. These flow times were monitored by electrical contacts in the mercury manometer, which permitted the recording of the intervals between the mercury meniscus dropping past successive contacts. The timing was carried out by a BBC microcomputer with a calibrated internal clock, connected to the pointers via a multiplexing interface.

The argon and argon/carbon dioxide mixtures used in the experiments were obtained from Air Products Ltd. The compositions of the mixtures were determined by gravimetric analysis by the suppliers, as shown in Table I. Measurements with a precision mass density balance confirmed these analyses.

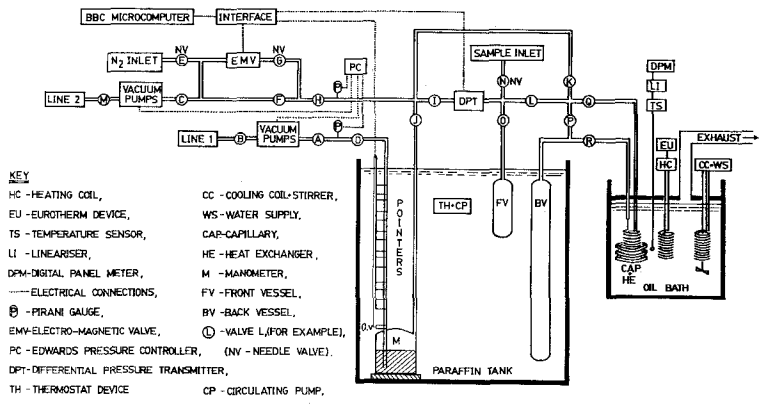

Fig. 1. The capillary flow viscometer apparatus.

Table I. Composition of Pure Gases and Gas Mixtures

Gas (nominal % Ar; balance CO_2)	Composition	
	% wt Ar	% wt CO_2
25% Ar	0.2507	0.7493
50% Ar	0.5003	0.4997
75% Ar	0.7497	0.2503

Various corrections were made to the flow times to allow for the effects of curved pipe flow, kinetic energy effects, gas imperfections, and slip flow [15]. These correction terms were minimized by the careful choice of the dimensions of the capillary tube and of the pressure settings. After the corrections had been made, the ratios of the argon–carbon dioxide mixture flow times to those of the argon standard gas at the same temperature were obtained, which gave the corresponding viscosity ratios.

The values of the standard argon viscosities used are given in Table II. They can be expressed by the relation

$$\ln(\eta/\eta_0) = A \ln(T/T_0) + B/T + C/T^2 + D \tag{1}$$

where $\eta_0 = 1\ \mu\text{Pa} \cdot \text{s}$, $T_0 = 1$ K, and the coefficients are as listed in Table III [18].

3. MIXTURE AND INTERACTION VISCOSITIES

Experiments were carried out at five temperatures for the Ar/CO_2 mixture of nominal mole fraction 0.5 and at two of these temperatures for the mixtures with nominal mole fractions 0.25 and 0.75. The resulting mixture viscosities η_{mix} are given in Table II and, by reason of a previous error analysis [15], are considered accurate to better than 0.7%. The carbon dioxide viscosities η_{22} are reported elsewhere [15] and are expressed by Eq. (1) with coefficients as listed in Table III. Mixture viscosities were plotted as a function of the mole fraction of the component gases at each of the five experimental temperatures, as shown in Fig. 2. The dashed lines in Fig. 2 are linear interpolations between the mixtures of the pure components [15, 18]. It can be seen that the present mixture viscosities are consistently less than these interpolations, and as expected [19] there are no viscosity maxima or minima.

In the study of the low-density binary mixture of two gases of molecular masses m_1 and m_2, it is convenient to interpret the results in

Table II. Viscosities of Argon–Carbon Dioxide Mixtures

Temp. (K)	T^*	A_{12}^* (BBMS)	η_{Ar} (μPa · s)	η_{CO_2} (μPa · s)	X_{Ar} (mole fraction)	η_{mix} (μPa · s)	η_{12} (μPa · s)	$\bar{\eta}_{12}$ (μPa · s)	% diff. $(\eta_{12}-\bar{\eta}_{12})$
301.0	1.652	1.103723	22.765	15.101	0.0000	15.101			
					0.2693	16.912	18.877		−0.846
					0.5245	18.775	18.843	19.038	−1.024
					0.7674	20.947	19.393		+1.865
					1.0000	22.765			
341.9	1.876	1.102987	25.277	17.075	0.0000	17.075			
					0.5245	21.204	21.455	21.455	
					1.0000	25.277			
401.3	2.202	1.103098	28.719	19.836	0.0000	19.836			
					0.5245	24.127	24.183	24.183	
					1.0000	28.719			
471.7	2.589	1.104401	32.536	22.926	0.0000	22.926			
					0.2693	25.218	27.694		−0.360
					0.5245	27.829	28.125	27.794	+1.191
					0.7674	29.993	27.563		−0.831
					1.0000	32.536			
521.0	2.859	1.105749	35.066	24.976	0.0000	24.976			
					0.5245	30.027	30.220	30.220	
					1.0000	35.066			

Table III. Coefficients of the Curve $\ln(\eta/\eta_0) = A \ln(T/T_0) + B/T + C/T^2 + D$, for the Argon Standard, Pure Carbon Dioxide, and Argon–Carbon Dioxide Interaction Viscosities

Gas	T (K)	A	B (K)	C (K^2)	D
Argon	60–2000	0.59077	−92.577	2990.4	0.0282
Carbon dioxide	198–1497	0.44973	−275.34	17660.0	0.86793
η_{12}	200–700	0.60988	−115.05	5095.6	−0.20728

terms of the so-called interaction viscosity η_{12}, which is the hypothetical viscosity of a gas of mass $2\mu = 2m_1m_2/(m_1+m_2)$ in which only unlike interactions take place. Within the first approximation of the Chapman–Enskog formulation, interaction viscosities may be calculated [1] from a knowledge of the viscosities of the mixture and its pure components at the same temperature, together with a dimensionless quantity A^*_{12} which is the ratio of two collision integrals,

$$A^*_{12} = \frac{\Omega^{(2,2)*}}{\Omega^{(1,1)*}} \tag{2}$$

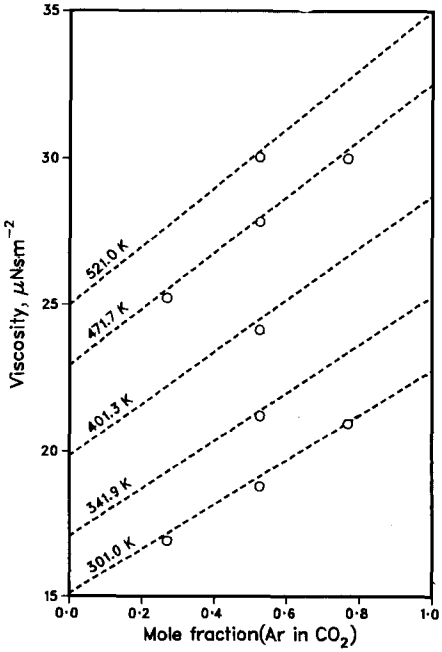

Fig. 2. Viscosity of Ar/CO_2 mixtures: ○, present work; ----, linear interpolations between pure components.

Values of A_{12}^* are relatively insensitive to the potential function used to calculate them. We have employed the BBMS function [20], which gives an accurate representation of the intermolecular forces of argon, to calculate the values given in Table II. A_{12}^* is a function of reduced temperature $T^* = kT/\varepsilon$, where k is the Boltzmann constant. Thus an estimate of the well depth ε_{12} is also required in the calculation of interaction viscosities. In the present work, we have used $\varepsilon_{12} = 182.2$ K, derived from the harmonic mean combining rule $\varepsilon_{12} = 2\varepsilon_{11}\varepsilon_{22}/(\varepsilon_{11} + \varepsilon_{22})$ [21]. ε/k for Ar and CO_2 were 142 and 252.7 K, respectively, these being the values from the BBMS potential for argon [20] and our analysis of carbon dioxide results [16]. Interaction viscosities were calculated for mixtures at all five temperatures, and averages made where more than one gas mixture was measured. The η_{12} values were not completely independent of composition at a given temperature owing to uncertainties in the viscosity measurements and mole fractions and deficiencies in the first-order kinetic theory expression used in the calculations. Changes of 1% in η_{11}, η_{22}, η_{mix}, and A_{12}^*, respectively, cause changes in η_{12} of the order of 0.5, 0.5, 2, and <0.01%. On the basis of this sensitivity and the spread on η_{12} values shown in Table II, the final η_{12} values are considered to be accurate to better than ± 1.9%.

4. INVERSION OF INTERACTION VISCOSITIES

Interaction viscosities may be inverted [1] to give an isotropic potential energy function corresponding to the unlike-pair interactions. However, to carry out this inversion, data are required over a larger temperature range than we have studied. To extend the range, therefore, pseudo experimental points were added to each end of the experimentally based interaction viscosities, to extend the temperature range from 301–521 to 200–700 K, as shown in Fig. 3 and Table V. The points were plotted on the basis of the heuristic equation $\eta_{12} = \eta_{11} + 0.515\ (\eta_{22} - \eta_{11})$, which fits the known data in the temperature range 301–521 K with a rms deviation of 0.62%. (This and all other rms deviations are based on averages over $n-1$ data points.) The interaction viscosities over the range 200–700 K were then inverted. The inversion procedure is an iterative process, and previous studies have demonstrated that the calculated viscosities usually converge onto the experimental viscosities through three iterations, after which there is no further improvement. In the present case, viscosities calculated from the second iteration potential had a lower rms deviation over the experimental temperature range, whereas the third iteration potential gave viscosities with a lower rms deviation over the experimental and pseudoexperimental range together. These rms deviations and the charac-

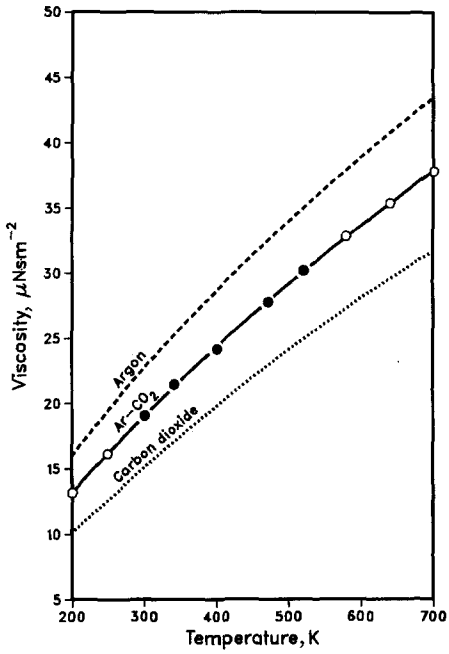

Fig. 3. Temperature dependence of Ar, Ar–CO_2, and CO_2 viscosities.

teristic parameters of these potentials are given in Table IV. The third iteration is shown in Figure 4, in the scale of which both the second and the third iterations are indistinguishable. The central solid portion of the potential energy function covers the range of separations r which arise from inversion of results over the experimental temperature range. At each end of this solid curve is a dashed region which corresponds to the pseudoexperimental temperature range. Figure 4 also shows the points at which further extrapolations have been added to the pseudoexperimental regions. These extrapolations, shown as continuations of the dashed curves at each end of the function, are in the form of a scaled BBMS potential [20].

Table IV. Characteristic Parameters and Viscosity Deviations of Ar–CO_2 Potentials

				rms viscosity deviation (%)	
Iteration No.	ε/k (K)	σ (nm)	r_{min} (nm)	301–521 K	200–700 K
2	182.2	0.35803	0.40058	0.2008	0.6602
3	182.2	0.35858	0.39986	0.3038	0.5414

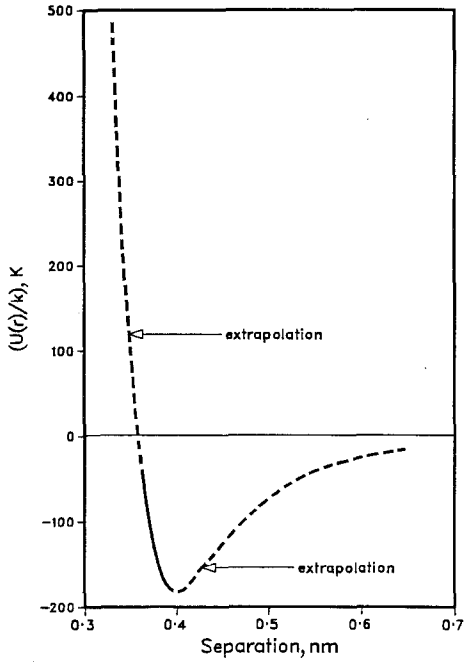

Fig. 4. Third iteration of Ar–CO_2 potential energy function.

Figure 5 shows an enlargement of the well region, and the extent of difference between the second and the third iteration potentials. When adding an extrapolation which is a scaling of a different potential function, there will be a discontinuity in the first and higher derivatives if the two functions have different gradients at the point of join. As seen in Fig. 5, these discontinuities are minor in the present instance.

5. COMPARISON WITH OTHER WORKERS' RESULTS

A comparison between the present results and those of other workers is shown in Table V. The η_{12} values calculated by Maitland et al. [8] can be seen to agree particularly closely around room temperature but are outside our range of experimental uncertainty of 1.9% above 500 K. The greatest discrepancy is −2.32%, and the rms deviation is 1.47%.

Kestin and Ro have carried out viscosity measurements on the Ar/CO_2 system ("meas." in Table V) [2]. The mixture viscosities are at different temperatures and compositions from the results presented here, and

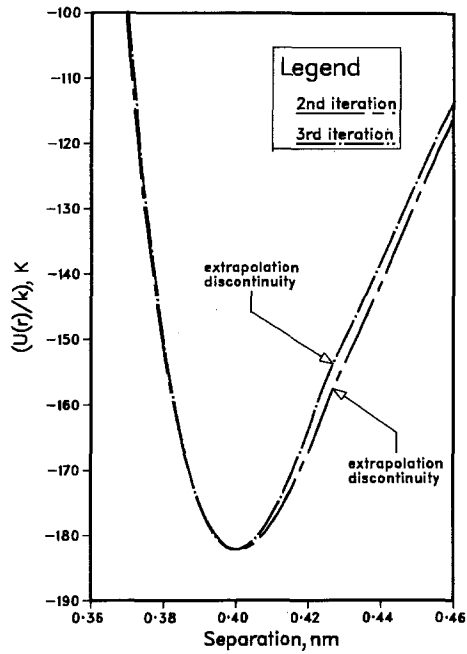

Fig. 5. Well region of second- and third-interaction potential energy function of Ar–CO_2.

it is therefore difficult to compare them directly. Their mixture viscosities, together with their measurements of pure Ar viscosity and out interpolation of their measurements of pure CO_2 viscosity, have therefore been used to calculate interaction viscosities, which are compared with the values presented here. The comparison is restricted to the temperatures quoted by Kestin and Ro which lie within the temperature range of 200–700 K. It can be seen that the results agree with ours to within 3.1% between 300 and 400 K and very closely with ours near 700 K, with an rms deviation of 2.15%.

Kestin and Ro have also carried out calculations based on the extended law of corresponding states developed by Kestin, Ro, and Wakeham (KRW) [3]. These agree with our interaction viscosities to within 2.7%, with a rms deviation of 2.24%.

Values of $p \cdot D_{12}$ are calculated from our interaction viscosities [1], using the relation

$$p \cdot D_{12} = \frac{3 \cdot \eta_{12} \cdot A^*_{12} \cdot R \cdot T}{5 \cdot \mu} \tag{3}$$

Table V. Comparison of η_{12} Values with Other Workers'

Temp. (K)	This work		Maitland et al. [8]		Kestin and Ro [2, 3]			
	A_{12}^* (2nd itn.)	η_{12} (μPa·s)	η_{12} (μPa·s)	Diff. (%)	η_{12} (μPa·s) (meas.)	Diff. (%)	η_{12} (μPa·s) (KRW)	Diff. (%)
200.00	1.119861	13.147	13.24	+0.71				
260.00	1.116540	16.723	16.71	−0.08				
298.15	1.115291	18.897			19.30	+2.13	19.40	+2.66
300.00	1.115247	19.000	18.91	−0.47				
323.15	1.114859	20.276					20.79	+2.54
348.15	1.114689	21.622					22.13	+2.35
360.00	1.114692	22.248	22.05	−0.89				
373.15	1.114778	22.936			23.64	+3.07	23.41	+2.07
400.00	1.115016	24.313	24.03	−1.16				
473.15	1.116517	27.906			28.49	+2.09	28.26	+1.27
500.00	1.117277	29.171	28.69	−1.65				
573.15	1.119603	32.490			32.64	+0.46		
600.00	1.120527	33.666	32.98	−2.98				
673.15	1.123123	36.766			36.74	−0.07	36.70	−0.18
700.00	1.124089	37.869	36.99	−2.32				
rms deviation				1.47%		2.15%		2.24%

On the basis of this equation, and the insensitivity of A_{12}^* to potential functions as mentioned previously, the experimental uncertainty in $p \cdot D_{12}$ is considered to be the same as for η_{12}, i.e., a maximum of 1.9%. Table VI shows the differences between our values and corresponding data calculated by Maitland et al. The differences are outside the range of experimental uncertainty above 360 K. The maximum difference is −2.84%, and the rms deviation is 1.98%. Also shown are comparisons with $p \cdot D_{12}$ data of Kestin and Ro [3], derived from measurements of viscosity ("meas.") and their extended corresponding-states calculation (KRW). The former agree to within our experimental uncertainty up to 473 K, and the latter up to 373 K, but both deviate by up to 2.99% above this. The rms deviations are 1.97 and 1.70%, respectively.

Interaction second virial coefficients B_{12} have been calculated from the present potential energy function using the relation [1]

$$B_{12}(T) = -2\pi N_A \int_0^\infty \{\exp[-U(r)/kT] - 1\} r^2 \, dr \tag{4}$$

in which N_A is Avogadro's number. It can be seen from Fig. 6 that these are in good agreement with experiment [22–26]. The agreement is much

Table VI. Comparison of $p \cdot D_{12}$ with Other Workers'

Temp. (K)	This work		Maitland et al. [8]		Kestin and Ro [2, 3]			
	A_{12}^* (2nd itn.)	$p \cdot D_{12}$ ($N \cdot s^{-1}$)	$p \cdot D_{12}$ ($N \cdot s^{-1}$)	Diff. (%)	$p \cdot D_{12}$ ($N \cdot s^{-1}$) (meas.)	Diff. (%)	$pm \cdot D_{12}$ ($N \cdot s^{-1}$) (KRW)	Diff. (%)
200.00	1.119861	0.70149	0.6973	−0.60				
260.00	1.116540	1.15654	1.145	−0.99				
298.15	1.115291	1.4970			1.490	−0.47	1.490	−0.47
300.00	1.115247	1.5144	1.495	−1.28				
323.15	1.114859	1.7402					1.733	−0.41
348.15	1.114689	1.9990					1.986	−0.65
360.00	1.114692	2.1269	2.091	−1.69				
373.15	1.114778	2.27293			2.26967	−0.14	2.24941	−1.04
400.00	1.115016	2.58333	2.534	−1.90				
473.15	1.116517	3.51203			3.47544	−1.04	3.44504	−1.91
500.00	1.117277	3.88224	3.788	−2.42				
573.15	1.119603	4.96695			4.85345	−2.29		
600.00	1.120527	5.39219	5.239	−2.84				
673.15	1.123123	6.62189			6.42399	−2.99	6.42399	−2.99
	rms deviation			1.98%		1.97%		1.70%

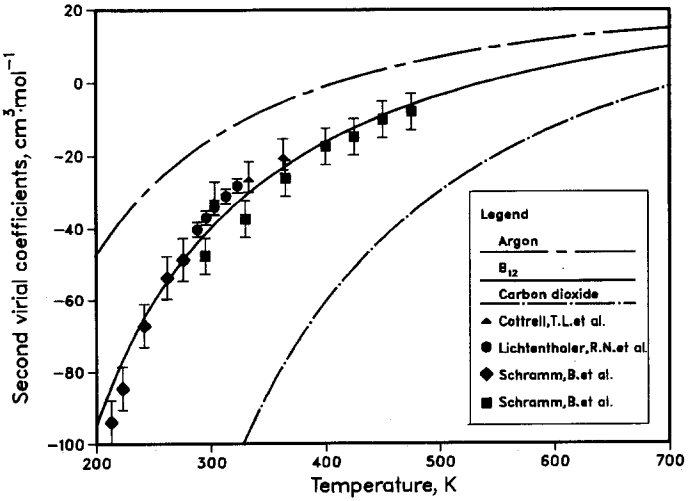

Fig. 6. Comparison of second virial coefficients with experimental data.

Table VII. Numerical Values for Second- and Third-Iteration Potentials

2nd iteration		3rd iteration	
r (nm)	U(r) (K)	r (nm)	U(r) (K)
0.21482	0.2870×10^5	0.21515	0.2820×10^5
0.25062	0.1075×10^5	0.25101	0.1056×10^5
0.28642	3453.0	0.28687	3393.0
0.31276	1207.0	0.31271	1215.0
0.31634	1023.0	0.31630	1030.0
0.31992	860.4	0.31989	867.6
0.32350	717.1	0.32347	724.2
0.32708	591.3	0.32706	598.2
0.33066	481.2	0.33063	487.8
0.33424	385.2	0.33423	391.6
0.33782	301.8	0.33781	307.9
0.34140	229.7	0.34140	235.4
0.34498	167.5	0.34499	173.0
0.34856	114.2	0.34857	119.4
	Extrapolation		
0.34856	114.2	0.34857	119.4
0.35096	82.99	0.35098	88.24
0.35359	52.46	0.35361	57.99
0.35649	17.80	0.35650	23.78
0.35969	−17.71	0.35971	−11.96
0.36327	−51.85	0.36328	−46.77
0.36729	−84.09	0.36731	−79.95
0.37186	−113.7	0.37188	−110.7
0.37711	−139.8	0.37713	−138.1
0.38322	−161.0	0.38324	−160.4
0.38491	−165.3	0.38493	−165.0
0.38667	−169.2	0.38669	−169.1
0.38851	−172.7	0.38853	−172.8
0.39044	−175.7	0.39045	−175.9
0.39245	−178.1	0.39246	−178.4
0.39456	−180.0	0.39457	−180.3
0.39678	−181.4	0.39679	−181.6
0.39910	−182.1	0.39911	−182.2
0.40155	−182.1	0.40155	−182.0
0.40412	−181.6	0.40413	−181.1
0.40684	−180.3	0.40684	−179.5
0.40970	−178.3	0.40971	−117.0
0.41274	−175.6	0.41274	−173.8
0.41595	−172.1	0.41595	−169.7
0.41935	−168.0	0.41935	−164.8
0.42296	−163.1	0.42296	−159.0
0.42680	−157.4	0.42680	−153.7

Table VII (*Continued*)

2nd iteration		3rd iteration	
r (nm)	U(r) (K)	r (nm)	U(r) (K)
		Extrapolation	
0.43088	−152.6	0.43088	−149.0
0.44878	−130.0	0.44881	−127.1
0.46668	−108.3	0.46674	−105.9
0.48458	−88.88	0.48467	−86.99
0.50248	−72.15	0.50260	−70.63
0.52038	−58.21	0.52052	−56.99
0.53828	−47.13	0.53845	−46.13
0.55619	−38.69	0.55638	−37.84
0.57409	−32.27	0.57431	−31.55
0.59199	−27.15	0.59224	−26.54
0.60989	−22.82	0.61017	−22.31
0.62779	−19.05	0.62810	−18.63
0.64569	−15.79	0.64603	−15.45
0.66359	−13.06	0.66396	−12.78
0.89507	−1.684	0.89645	−1.635
1.07408	−0.5491	1.07574	−0.5334

better than that obtained by both Pack et al. [4] and Hough and Howard [10] and better than predicted by Maitland et al. [8]. The reproducibility of second virial coefficients is in accord with the findings of Smith and Tindell [27], who identified similar isotropic potential functions relating to viscosities and second virial coefficients.

6. CONCLUSION

It has been shown that interaction viscosities presented here agree closely with the experimental data of Kestin et al. above 500 K and with the theoretical calculations of Maitland et al. at lower temperatures, our own data lying between the sets of comparison data. The binary diffusion coefficients of this work agree closely with both the theoretical calculations of Maitland et al. and the calculations of Kestin and Ro at low temperatures but deviate increasingly with temperature. It is difficult to identify any unambiguous trend from these comparisons.

Second virial coefficients calculated from our isotropic pair potential

energy function agree closely with experimental values and suggest that an isotropic potential energy function can be a useful approximation even for a system as anisotropic as Ar/CO_2.

ACKNOWLEDGMENTS

A. Townsend acknowledges receipt of a SERC studentship. The authors thank I. N. Hunter of the Physical Chemistry Laboratory, University of Oxford, for carrying out the mass density balance determinations. A Scott of the National Engineering Laboratory, East Kilbride, U.K., is thanked for his interest in and advice on this project.

REFERENCES

1. G. C. Maitland, M. Rigby, E. B. Smith, and W. A. Wakeham, *Intermolecular Forces* (Clarendon Press, Oxford, 1981), Chaps. 5, 6, and 9.
2. J. Kestin and S. T. Ro, *Ber. Buns.-Gesell.* **78**:20 (1974).
3. J. Kestin and S. T. Ro, *Ber. Bunsen.-Gesell.* **80**:619 (1976).
4. G. A. Parker, R. L. Snow, and R. T. Pack, *J. Chem. Phys.* **64**:1668 (1976).
5. R. K. Preston and R. T. Pack, *J. Chem. Phys.* **66**:2480 (1977).
6. G. A. Parker and R. T. Pack, *J. Chem. Phys.* **68**:1585 (1978).
7. R. T. Pack, *Chem. Phys. Lett.* **55**:197 (1978).
8. G. C. Maitland, M. Mustafa, V. Vesovic, and W. A. Wakeham, *Mol. Phys.* **57**:1015 (1986).
9. A. M. Hough and B. J. Howard, *J. Chem. Soc. Faraday Trans. 2* **83**:173 (1987).
10. A. M. Hough and B. J. Howard, *J. Chem. Soc. Faraday Trans. 2* **83**:191 (1987).
11. J. M. Hutson and B. J. Howard, *Mol. Phys.* **45**:769 (1982).
12. J. M. Hutson, *J. Chem. Phys.* **81**:2357 (1984).
13. B. J. Howard and A. S. Pine, *Chem. Phys. Lett.* **122**:1 (1985).
14. J. M. Hutson, *J. Chem. Soc. Faraday Trans. 2* **82**:1163 (1986).
15. L. Delauney, G. P. Matthews, and A. Townsend, *J. Phys. E Sci. Instrum.* **21**:890 (1988).
16. G. P. Matthews and A. Townsend, *Chem. Phys. Lett.* **155**:518 (1989).
17. G. C. Maitland, V. Vesovic, and W. A. Wakeham, *Mol. Phys.* **54**:287 (1985).
18. G. C. Maitland and E. B. Smith, *J. Chem. Eng. Data* **17**:150 (1972).
19. J. O. Hirschfelder, M. H. Taylor, T. Kihara, and R. Rutherford, *Phys. Fluids* **4**:663 (1961).
20. G. C. Maitland and E. B. Smith, *Mol. Phys.* **22**:861 (1971).
21. B. E. Fender and G. D. Halsay, Jr., *J. Chem. Phys.* **36**:1881 (1962).
22. J. H. Dymond and E. B. Smith, *The Virial Coefficients of Pure Gases and Mixtures* (Clarendon Press, Oxford, 1980), pp. 260–261.
23. T. L. Cotterell, R. A. Hamilton, and R. P. Taubinger, *Trans. Faraday Soc.* **52**:1310 (1956).
24. R. N. Lichtenthaler and K. Schafer, *Ber. Bunsenges. Phys. Chem.* **73**:42 (1969).
25. B. Schramm and R. Gehrmann, Unpublished, as reported in Ref. 22 (1979).
26. B. Schramm and H. Schmiedel, Unpublished, as reported in Ref. 22 (1979).
27. E. B. Smith and A. R. Tindell, *Faraday Disc. Chem. Soc.* **73**:221 (1982).